EQUALIZATION OF TWO-PATH FADING: AN ANALYSIS FOR VARIOUS DIGITAL MODULATION TECHNIQUES

K. Metzger and R. Valentin
Forschungsinstitut der Deutschen Bundespost
D-6100 Darmstadt
Federal Republic of Germany

1. Introduction

The performance of digital radio systems is severely impaired by frequency-selective fading. One countermeasure against distortions is the use of adaptive equalizers. This paper presents the results of a computer simulation of IF equalizers and baseband equalization for the following types of modulation: Offset-Quadrature-Phase-Shift-Keying (OQPSK), Quadrature-Partial-Response Signalling (QPRS) and 16-Quadrature-Amplitude-Modulation (16-QAM). The results are depicted by means of the "signature curves" /1/ of the investigated modulation schemes, because most frequency-selective fading events can be described in a limited bandwidth ($\Delta f<50$ MHz) by an effective two-path-model. These curves show -for a two-path fading event with relative amplitude b and delay time τ of the indirect path- the dependence of notch depth $\lambda=20_{10}\log(1-\varkappa)$ on notch frequency f_N for a fixed bit error rate of 10^{-3}. The symbol $\varkappa$ denotes b for b<1 (minimum phase fade) and 1/b for b>1 (non-minimum phase fade). The calculations are based on perfect Nyquist filtering with raised-cosine frequency characteristic (16-QAM, OQPSK) or cosine frequency characteristic (QPRS), and include simulation of the carrier and timing recovery circuits as described in a former paper /2/. In the examples presented in the following, the delay time has the value $\tau = 6$ ns and the ratio of τ and the symbol period T is kept fixed for the different types of modulation thus determining the transmitted bit rate. The roll-off-factor for the QAM and PSK systems is assumed to be $\alpha = 0.5$.

2. IF equalizer

2.1 Slope equalizer

The simplest IF equalizer cancels the slope of the channels amplitude characteristic between two predetermined frequency points f_c-f_s and f_c+f_s, where f_c denotes the carrier frequency. The transfer function of the equalizer is therefore

$$H_{eqs}(f) = 10^{af} \tag{1}$$

with $a=\left[A_c(f_c-f_s)-A_c(f_c+f_s)\right]/(40f_s)$ and with $A_c(f)=20_{10}\log|H_c(f)|$ denoting the insertion loss of the channel with the transfer function $H_c(f)$. Slopes of the amplitude characteristic occur, if the notch lies outside but close to the transmitted frequency band. Notches in this region mainly affect the more complicated types of modulation. Hence, slope equalizers are more useful for 16-QAM systems than for the lower level types of modulation. Figs. 1 and 2 show examples of calculated signatures for a 70-Mbit/s OQPSK-system and for a 140-Mbit/s 16-QAM system with slope equalizers designed for different sampling points $f_s=k/(2T)$. With the notch being within the transmitted band, the performance may even be impaired for the simpler modulation system (Fig.1), if the value of k is not chosen properly.

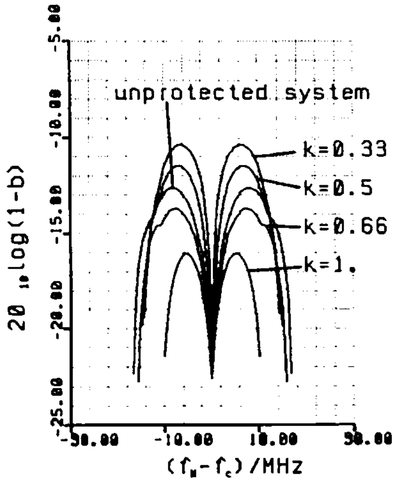

Fig. 1: Signatures of a 70-Mbit/s OQPSK-system without and with slope equalizer, $f_s=k/(2T)$: equalized frequency points

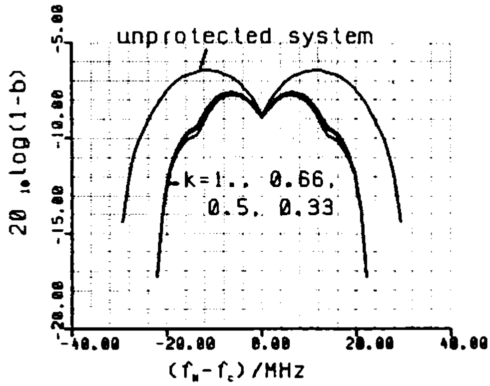

Fig. 2: Signatures of a 140-Mbit/s 16-QAM system without and with slope equalizer

2.2 Resonance equalizer

Attenuation notches near the carrier frequency can be better equalized by means of a parallel resonance circuit, which is adapted with its resonance frequency and quality factor to flatten the amplitude characteristic of the channel at n sampled frequency points (in the calculations we chose n=5). Moreover, the phase characteristic of the resonance circuit tends to cancel the group-delay distortion of the channel for minimum phase fades as well, so that an almost perfect equalization is achieved. For non-minimum phase fades the phase characteristic of the equalizer increases the channels group-delay distortion, so that the overall performance of the system is improved only slightly. The Fig. 3 shows the signature for a 70-Mbit/s QPRS-system, once unprotected and once with a resonance equalizer for $b>1$. The lacking symmetry of the signature with equalization is due to the non-symmetric transfer function of the resonance circuit. Fig. 4 shows the eye pattern for the event that corresponds to the cross in Fig. 3. The calculated timing instant t_n is indicated by an arrow, which coincides with maximum eye opening. The solid vertical line gives maximum eye opening for the undistorted system and indicates that the severe phase distortion of channel and equalizer causes a delay of $0.66 \cdot T$. The horizontal line denotes the threshold at the decision element.

2.3 Equalization of linear and quadratic amplitude distortions

We now investigate a slope equalizer followed by an equalizer which removes quadratic amplitude distortions. Such an equalizer can be realized by means of a resonance circuit, whose resonance is fixed to the carrier frequency. Its quality factor is adjusted to equalize the amplitude characteristic at $f=f_c$ and at $f=f_s$ (see 2.1). Its network should be a shunt circuit for "concave" amplitude distortions ($|H_c(f_c)\,H_{eqs}(f_c)| < |H_c(f_s)\,H_{eqs}(f_s)|$) and a series circuit for "convex" amplitude distortions (reversing the "<" sign above). Fig. 5 shows calculated and measured /3/ sig-

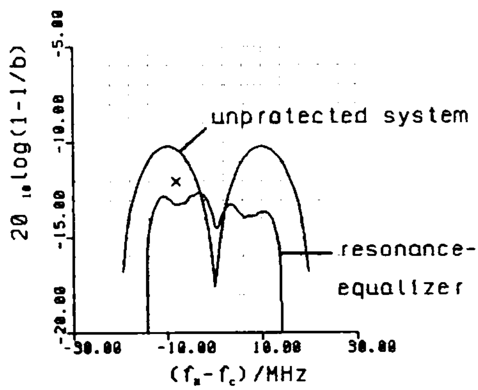

Fig. 3: Signature of a 70-Mbit/s QPRS-system with resonance equalizer (b>1)

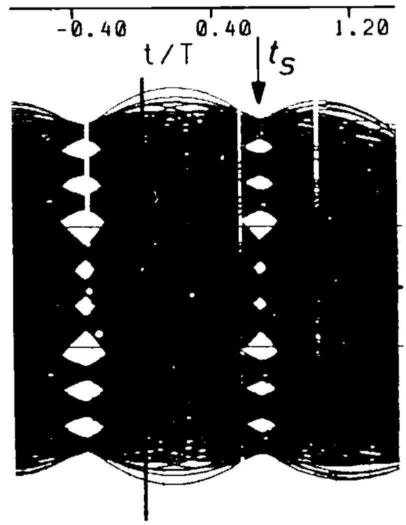

Fig. 4: Eye diagram of the system of Fig. 3 and a fading event corresponding to point x.

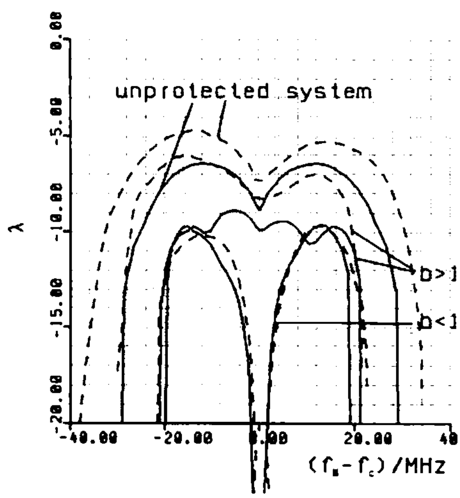

Fig. 5: Signatures of a 140-Mbit/s 16-QAM system with slope and quadratic equalizer
--- measured
—— calculated

natures of a 140-Mbit/s 16-QAM system with slope and quadratic equalization for b<1 and b>1.

3. Baseband equalizer

We investigated linear tapped delay-line equalizers, which minimize the peak distortion of the received overall impulse response p(t) by use of the zero forcing algorithm. The equalized impulse response $p_{eq}(t)$ is

$$p_{eq}(t) = \sum_{k=-n}^{+n} \gamma_k p(t+kT), \qquad (2)$$

where 2n+1 is the number of taps with complex tap gains γ_k, which are adjusted such that

$$p_{eq}(t_s+kT) = \delta_0^k \qquad \text{for } k \leq n \qquad (3)$$

with δ_0^k denoting the Kronecker symbol.

The Fig. 6 shows the signatures of a 140-Mbit/s 16-QAM system with 3,5,7 and 9 taps. The ripples in the computed signatures are due to fast changes of the tap gains with a change of notch-frequency and due to the amplitude modulated part of

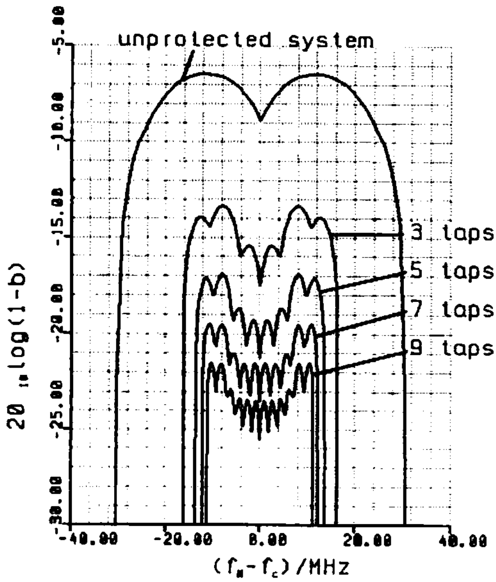

Fig. 6: Signatures of a 140-Mbit/s 16-QAM system with linear tapped delay-line equalizers

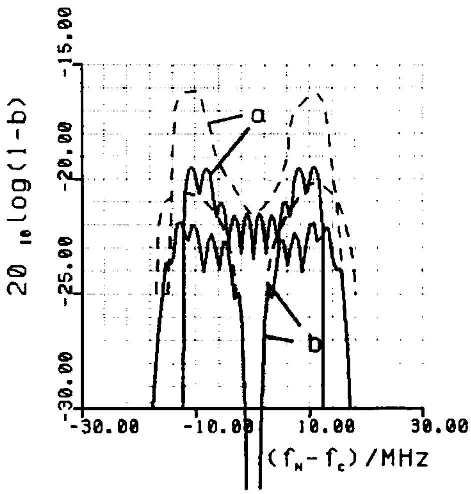

Fig. 7: Signatures of a 140-Mbit/s 16-QAM system
(a) 7-tap transversal equalizer
(b) additional slope and quadratic equalizer
--- measured
—— calculated

the 16-QAM signal. It can be shown by a first approximation that two adjacent minima of the ripples are separated by the distance

$$\Delta f \approx \frac{1}{4\tau} \frac{1-b}{1+b} \qquad (4)$$

In Fig. 7 are finally shown measured /3/ and calculated results for the signature of a 140-Mbit/s 16-QAM system and minimum phase fades ($b<1$). Curves (a) hold for a 7-tap transversal equalizer. The curves (b) apply to an additional slope and quadratic equalizer, which precedes the baseband equalization.

References

/1/ Emshwiller, M., "Characterization of the performance of PSK digital radio transmission in the presence of multipath fading", Int. Conf. Commun. (1978), Toronto, Ont., Canada, Paper 47.3

/2/ Metzger, K., Valentin, R., 1984, "Analysis of different digital modulation schemes using measured parameters of a two-path model", U.R.S.I. XXIst General Assembly, Florence, Abstracts p. 72

/3/ Nossek, J., A., et. al., paper to be published at ICC 1985.